Macromolecules

Cite This: Macromolecules 2019, 52, 4694−4702

Article

pubs.acs.org/Macromolecules

Influence of Short-Range Scrambling of Monomer Order on the Hydrolysis Behaviors of Sequenced Degradable Polyesters

Jamie A. Nowalk,[†] Jordan H. Swisher,[†] and Tara Y. Meyer*[,†,‡]

[†]Department of Chemistry, University of Pittsburgh, Pittsburgh, Pennsylvania 15260, United States

[‡]McGowan Institute for Regenerative Medicine, University of Pittsburgh, Pittsburgh, Pennsylvania 15219, United States

Supporting Information

ABSTRACT: The extent to which small changes in monomer sequence affect the behaviors of biological macromolecules is studied regularly, yet the dependence of bulk properties on small sequence alterations is underexplored for synthetic copolymers. Investigations of this type are limited by the arduous syntheses required, lack of scalability, and scarcity of examples of polymer systems that are known to exhibit sensitive sequence/property dependencies. Our group has previously explored the hydrolysis behaviors of a library of sequenced poly(lactic-*co*-glycolic acid)s and found a strong correlation with the L−G sequence. To investigate the degree to which properties are dominated in this system by relatively short-range sequence changes, we have incorporated precisely sequenced and mildly "scrambled" L−G oligomers into cyclic macromonomers and subjected them to entropy-driven ring-opening metathesis polymerization, a method that we have recently shown produces polymers with molecular weight control and sequence preservation. The resulting polymers, which have identical composition and molecular weight, were hydrolyzed. Molecular weight decrease, mass loss, thermal behaviors, and film/surface characteristics were monitored to reveal stark differences in degradation behaviors despite the confinement of errors within a short segment.

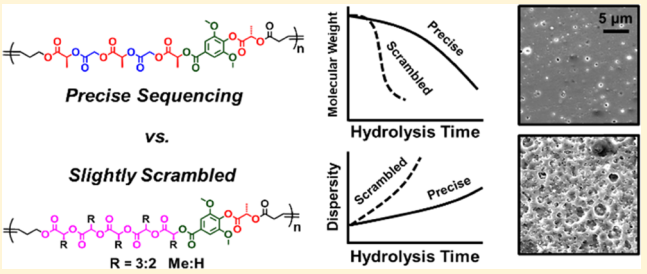

INTRODUCTION

In synthetic polymer science, there are few studies of the sensitivity of bulk properties to discrete changes in monomer sequence in an otherwise sequence-controlled polymer (SCP). The degree to which sequence plays a role in the macromolecular function is well established in nature and most appreciated within the scope of biological chemistry, where it is well understood that for some biopolymers a single monomer sequencing error can dramatically affect the function, e.g., DNA, while for others, the behavior is controlled by an overall sequence pattern rather than exact monomer identity and placement, e.g., structural proteins like spider silk.[1−3]

Although there has been an increasing effort in studying structure and function in SCPs,[4−6] little is known about the sensitivity of properties to sequence errors. Synthetic advances have aided in both the expansion in the number and types of SCPs[7−19] and the studies of the bulk properties,[20−24] solution properties,[16,21,25−32] and complex behaviors[33−40] of these materials. Still, there has been less effort to date in trying to understand the effects of sequence errors. One way to visualize sequence errors that is applicable to periodic copolymers of the type discussed herein is illustrated in Figure 1. In this model, the introduction of increasing numbers of errors to the base alternating sequence eventually yields a polymer with block lengths and block dispersities similar to those that would be obtained from a statistical polymerization. Based on this model, a variety of property responses can be envisioned. At one end of the continuum, a property could be found to behave like DNA, wherein even small numbers of errors cause

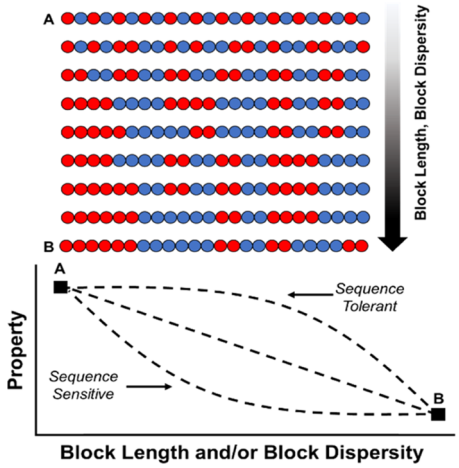

Figure 1. Range of bulk property/sequence tolerance profiles for random and sequence-controlled copolymers, where **A** represents a precisely alternating and **B** represents a statistically random copolymer.

Received: March 11, 2019
Revised: May 21, 2019
Published: June 11, 2019

DOI: 10.1021/acs.macromol.9b00480
Macromolecules 2019, 52, 4694−4702

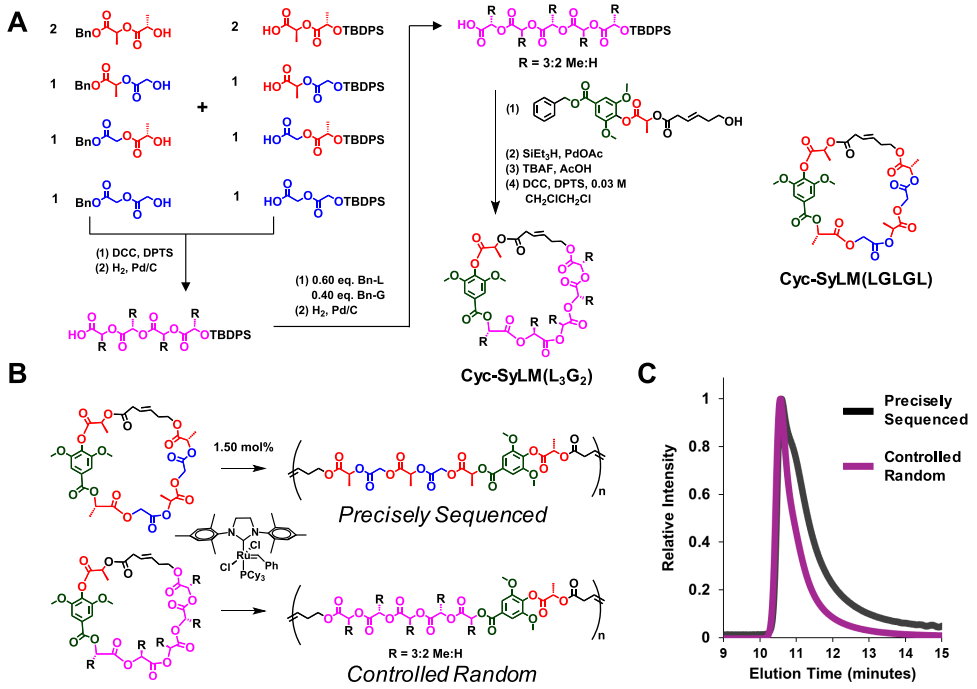

Figure 2. Synthesis of **Poly SyLM(L_3G_2)**: (A) synthesis of **Cyc-SyLM(L_3G_2)** macrocycle; (B) polymerization of macrocycles to produce precisely sequenced and controlled random copolymers of identical composition; and (C) size exclusion chromatography traces of both copolymers.

dramatic differences in the property (Figure 1, bottom curve). At the other, a base sequence could be found, as in structural proteins, to be resilient to the introduction of sequence mistakes, retaining the performance of the fully sequenced version despite a significant introduction of errors (Figure 1, top curve). The exact profile and the degree of dependence would, of course, be important to both improve sequence engineering for particular behaviors and allow more practical syntheses of semisequenced copolymers in systems in which errors can be tolerated.[21,33,41−45]

In this paper, we examine the effect of sequence on properties for a class of degradable polyesters closely related to poly(lactic-*co*-glycolic acid)s (PLGAs). PLGAs, which are widely used for bioengineering applications including drug delivery and cell growth scaffolding, are almost always random in sequence.[46−54] Random PLGAs such as **PDLGA-50** are traditionally prepared from the ring-opening polymerization of lactide and glycolide, which, due to the reaction's statistical nature, typically results in a polymer with a wide distribution of block lengths. This distribution is important because it is known that G-rich regions degrade more rapidly than mixed or L-rich regions in an aqueous environment. As a result, polymer mass and molecular weight decrease rapidly upon exposure to water.[55] The degree of this hydrolytic susceptibility of fully random PLGAs is commonly controlled by altering the composition of the monomer feed. The average block length and thus degradation rates, however, are not dramatically affected until approximately 80−90% of the monomer feed composition is one monomer.[56−58]

Our group has invested significant effort in establishing hydrolysis behaviors as a function of sequence for PLGAs.[59−66] A library of SCPs comprising the three monomer units, s-lactic acid (**L**), R-lactic acid ($\mathbf{L_R}$), and glycolic acid (**G**), was previously studied. Hydrolysis was found to be sequence-dependent in all cases, and a dramatic difference was observed relative to random copolymers of the same compositions.[62,64] We previously reported property differences between alternating copolymer $(LG)_n$, which we termed **Poly LG**, and its random sequence analog **PDLGA-50** (and the stereopure variant **PLLGA-50**). The dramatic differences in hydrolysis behaviors between the alternating and random sequences present an opportunity to investigate the degree of property sensitivity to minor sequence alterations.

We sought to design a sequenced polyester with an alternating LG segment and study its degradation behaviors alongside a semiscrambled, or a controlled random, copolymer. This synthetic route was used, as opposed to preparing two precisely sequenced copolymers, to investigate the realm between sequenced and random. Our goal was to study the property tolerance of this family of polyesters to sequence errors and to search for unexpected, sequence-induced complex behaviors like those observed in our previous works.[59,62,64,66−68] We chose to prepare these polymers using entropy-driven ring-opening metathesis polymerization (ED-ROMP). Using this process, large macrocycles are ring-opened to form entropically favored linear chains with reproducible, controlled molecular weights.[69−71] Though these copolymers deviate in structure from pure PLGAs due to the necessary incorporation of the polymerizable olefin functionality, the realized molecular weight control is crucial to effectively make comparisons between polymers containing subtle differences in sequence.[60]

Herein, we describe the synthesis of a precisely sequenced polyester comprising **L**, **G**, syringic acid (**Sy**), a metathesis-active olefin linker (**M**), and a copolymer of identical monomer composition but with a slightly scrambled LG sequence. Syringic acid was incorporated into these copolymers to elevate the T_g above 37 °C, which is important for future applications.[72] Molecular weight decrease, mass loss, thermal properties, and film characteristics were monitored. Dramatic differences in the degradation behaviors of the two polymers

DOI: 10.1021/acs.macromol.9b00480
Macromolecules 2019, 52, 4694−4702

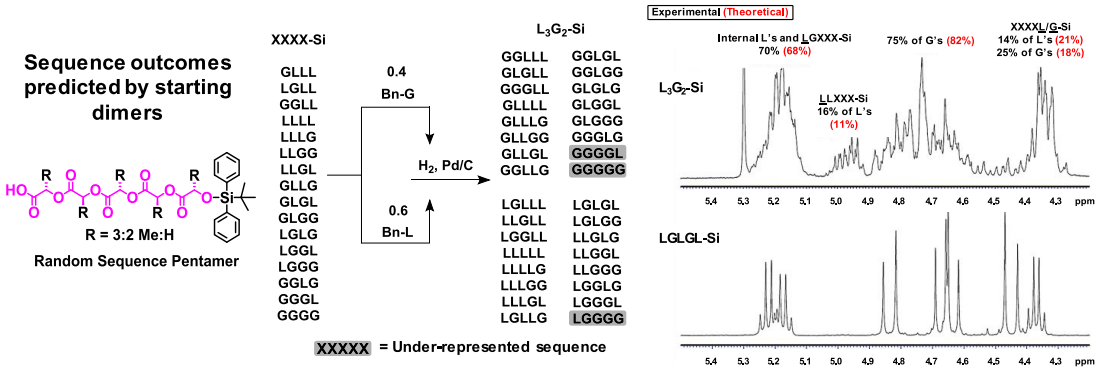

Figure 3. Theoretical and experimental sequence outcomes within the mixture of random $\mathbf{L_3G_2}$-**Si** pentamers prepared from precursor dimers and ^{1}H NMR spectroscopy (red labels are theoretical and black are experimental).

were observed, despite the relatively small differences in sequence.

RESULTS AND DISCUSSION

Synthesis of Sequence-Controlled Polymers. All L-monomers denoted in this work are the L-lactic acid isomer. Oligomers are named from the acid terminus to the alcohol terminus by listing each unit. The oligomer **SyLM(LGLGL)**, for example, consists of syringic acid−lactic acid−metathesis linker and an alternating sequence of three lactic acids and two glycolic acid units. A prefix of Cyc- is used to indicate the ring-closed macromonomer and Poly is used to indicate the ring-opened polymer.

The hydroxy-acid-sequenced oligomer **SyLM(LGLGL)** was prepared utilizing standard iterative ester-coupling techniques described by our group,[65,66] and the ring-closed species **Cyc-SyLM(LGLGL)** was obtained in good yield upon macrolactonization under dilute conditions, as described previously.[72] **Sy**, which introduces the largest structural deviation from a traditional aliphatic polyester such as PLGA, was incorporated as an inert, conformationally rigid unit to counteract the dramatic lowering of the glass transition temperature that results from the incorporation of the conformationally flexible metathesis linker **M**.[73−75]

As the first step in preparing a randomized analog to this macrocycle, **Cyc-SyLM($\mathbf{L_3G_2}$)**, a mixture of random pentamers comprising 60 mol % **L** and 40 mol % **G** (i.e., $\mathbf{L_3G_2}$) was prepared by the ester coupling of a mixture of monoprotected dimers: **Bn-LL**, **Bn-LG**, **Bn-GL**, **Bn-GG**, **LL-Si**, **LG-Si**, **GL-Si**, and **GG-Si** (Si = TBDPS, Bn = benzyl), followed by full benzyl hydrogenolysis and subsequent coupling with additional **Bn-L** (0.60 equiv) and **Bn-G** (0.40 equiv). The resulting **Bn-$\mathbf{L_3G_2}$-Si** was then deprotected once more via hydrogenolysis to yield the free acid pentamer $\mathbf{L_3G_2}$-**Si** (Figure 2). During the synthesis of these mixtures of compounds, significant differences in the polarity of the protected and unprotected species allowed for surprisingly uncomplicated purifications using column chromatography.

Randomized hydroxy-acid oligomer **SyLM($\mathbf{L_3G_2}$)** was prepared by coupling an acid-protected **Bn-SyLM** to the random alcohol-protected pentamer $\mathbf{L_3G_2}$-**Si** followed by sequential benzyl and silyl deprotection reactions. Macrocyclic oligomer **Cyc-SyLM($\mathbf{L_3G_2}$)** was then prepared utilizing the same macrolactonization technique described above (Figure 2A). Both cyclic species were then subjected to ED-ROMP at 0.7 M with 1.50 mol % Grubbs second-generation catalyst to obtain **Poly SyLM(LGLGL)** (M_n = 44.3 kDa, $Đ$ = 1.15) and **Poly SyLM($\mathbf{L_3G_2}$)** (M_n = 47.6 kDa, $Đ$ = 1.07) (Figure 2B,C). This synthetic approach yielded both the perfectly sequenced copolymer and the scrambled analog, wherein the disorder was confined to the LG-pentamer region of the otherwise precise copolymer. Each polymer's backbone contains the expected thermodynamic ratio from Grubbs II of ∼85% *trans*-olefin and ∼15% *cis*-olefin.

Sequence Characterization. The structure of **Poly SyLM(LGLGL)** was confirmed by comparison with previously acquired NMR spectroscopy and matrix-assisted laser desorption ionization time-of-flight (MALDI-ToF) mass spectrometry data.[72] The analysis shows that the sequence is preserved throughout all steps of the synthesis.

The structure of the random copolymer is more complex but can be confirmed by first analyzing the composition of the pentamers that are embedded. ^{1}H NMR spectroscopy and mass spectrometry show that the distribution in $\mathbf{L_3G_2}$-**Si** is consistent with the expected 32 sequence outcomes arising from the statistical combination of protected dimers (Figure 3).

While the complete assignment of the sequences is not possible, select signals of known monomer units, when compared to our large library of L/G-containing sequenced oligomers, allowed us to quantify to a degree the sequence outcomes. A terminal, deprotected L-methyne proton displays a resonance near 5.2 ppm unless the next unit in the sequence is another L, in which case, the signal shifts to 5.0 ppm. The theoretical composition of LLXXX-Si units is 11% of all Ls, whereas the ^{1}H NMR spectrum indicates 16% of Ls in this placement. Resonances for both L-methyne and G-methylene protons that are last in the pentameric sequences, adjacent to the silyl-protecting group (XXXX**L**/**G**-Si), appear at 4.35 ppm. Based on the L-units already accounted for and the integrations of the L-methyl resonances at 1.3 ppm, the signals displayed from L-units in this region were calculated to represent 14% of all Ls, whereas this theoretical value was 21%. The signals for G-units appear in one of two regions, either 4.5−4.9 ppm or in the 4.35 region (XXXX**G**-Si). The theoretical values compared to the experimental placements of Gs varied by 7%. Overall, these integrations are consistent with those expected. The differences likely correspond to a small degree of oligomer bond cleavage that occurred during the synthesis and isolation steps.

After ring closing, the sequences and monomer composition of both macrocycles were elucidated using ^{1}H NMR spectroscopy and high-resolution mass spectrometry (HRMS). The ^{1}H NMR spectra of the macrocycles are most

DOI: 10.1021/acs.macromol.9b00480
Macromolecules 2019, 52, 4694−4702

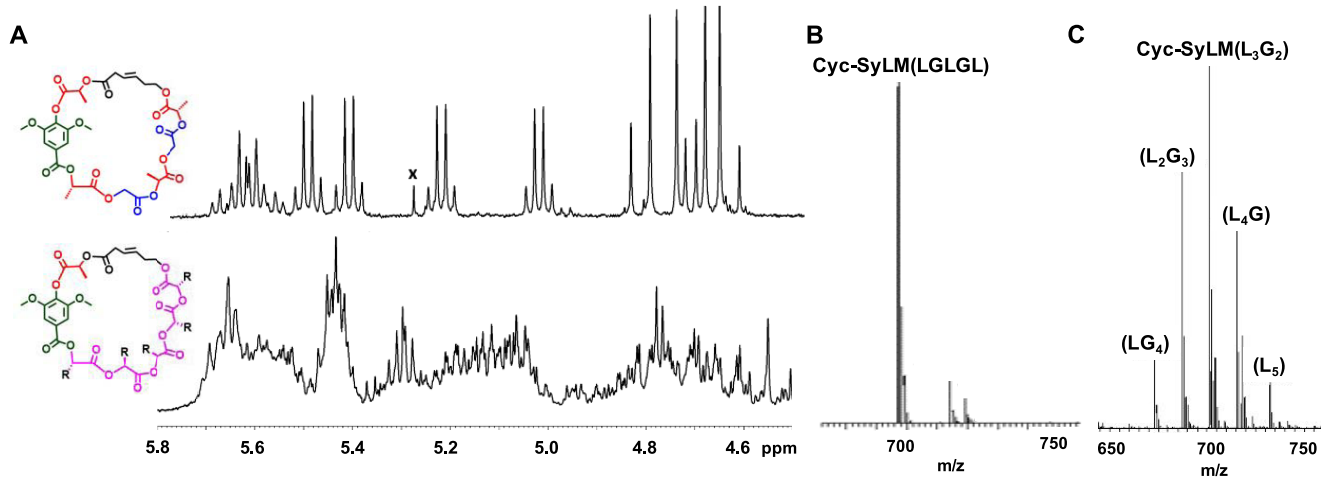

Figure 4. Sequence characterization of macrocycles: (A) ^{1}H NMR spectra of methyne, methylene, and olefin regions of **Cyc-SyLM(LGLGL)** and **Cyc-SyLM(L_3G_2)**; (B) high-resolution mass spectrum of **Cyc-SyLM(LGLGL)**; and (C) high-resolution mass spectrum of **Cyc-SyLM(L_3G_2)** macrocycle mixture.

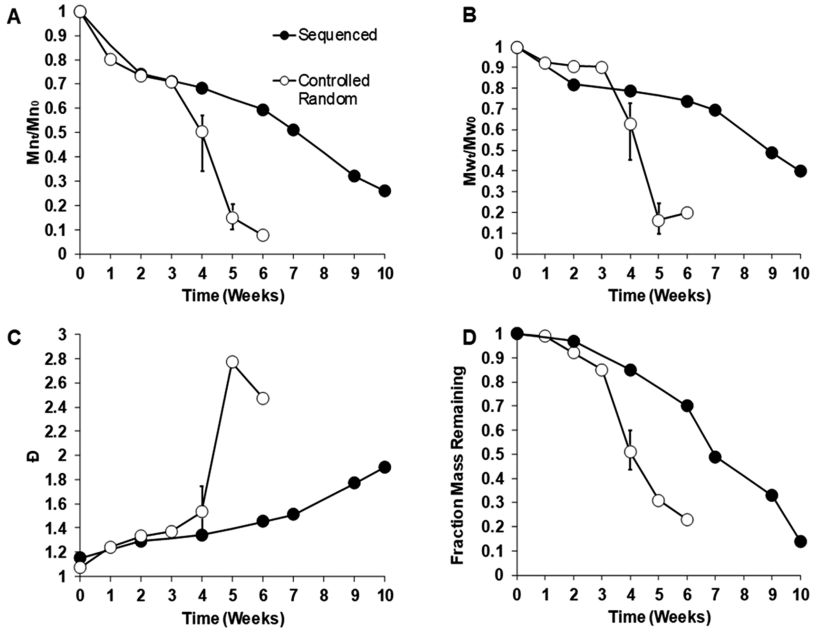

Figure 5. Molecular weight and mass loss profiles of **Poly SyLM(LGLGL)** and **Poly SyLM(L_3G_2)**: (A) number average molecular weight (M_n) loss over time; (B) weight average molecular weight (M_w) loss over time; (C) dispersity ($Đ$) over time; and (D) film mass loss over time. Range bars are included for sample sets with significant deviations (>0.1 on the *y*-axis).

informative in the 4.5−6.0 ppm region, where **G**-methylene, **L**-methyne, and **M**-olefin protons appear (Figure 4A). The sequenced macrocycle clearly displays four distinct quartets corresponding to the **L**-methyne protons, as well as two pairs of doublets from the **G**-methylene protons. Although this spectral region is complex for the controlled random macrocycle, the same subregions of **G**-methylene (4.5−4.9 ppm), **L**-methyne (5.0−5.5 ppm), and **M**-olefin protons (5.5−5.8 ppm) remain distinct. Further structural insights were obtained from the HRMS of both macrocycles. **Cyc-SyLM(LGLGL)** displayed a single major peak matching the theoretical mass (Figure 4B), whereas **Cyc-SyLM(L_3G_2)** displayed five peaks corresponding to the masses of macrocycles containing LG_4 to L_5 pentamers. The peak associated with a **Cyc-SyLM(G_5)** species was not observed, which confirms that this hydrolytically sensitive species did not survive the final steps in the synthesis (Figure 4C). Even without this sensitive macrocycle in the mixture, the overall monomer composition did not suffer dramatically. A synthetic target of a 3:2 L-to-G ratio resulted in an experimental ratio of 3:1.88 according to the ^{1}H NMR spectrum.

Film Casting. PLGAs may be processed into a variety of devices including high-surface-area scaffolds, microparticles, pellets, and films.[48,51−54,76] In our sequence/property investigations, we wished to produce uniform devices of small mass with high efficiency and found that solution casting of thick polymer films, or disks, was effective in this endeavor.[73] Thick films were cast on 1.25 cm glass coverslips,[77] and thicknesses were measured using optical profilometry (Figures S1 and S2). The 120−150 μm films were dried in a vacuum chamber, delaminated from the glass coverslips, and placed in phosphate

DOI: 10.1021/acs.macromol.9b00480
Macromolecules 2019, 52, 4694−4702

buffer solution upon the commencement of the hydrolysis study.

Hydrolysis. Samples were placed in a 10× phosphate buffer solution and incubated at 37 °C for the duration of the study. A preliminary molecular weight loss study was performed on a single film of both samples to determine time points for the full study. In the full study reported herein, three films were used for each molecular weight and mass data point, and averages were calculated. A single film was used for differential scanning calorimetry measurements and scanning electron microscopy (SEM) imaging. At a given time point, samples were removed from the buffer solution, blotted dry, frozen in liquid N_2, and lyophilized for 3 h to remove residual water. The pH of the buffer was monitored over time and remained unchanged for the duration of the study.

The ^{1}H NMR spectra of the lyophilized films over the course of the study showed neither a significant L/G composition change nor transesterification/sequence scrambling, similar to the previously studied sequenced PLGAs (see Supporting Information). It is notable that in fully random PLGAs, the L/G ratio increases over time, as G linkages are cleaved and short-chain oligomers are washed away.[52] ^{1}H NMR spectra of each copolymer in this study did show a decrease in **M**-content near the very end of the study, indicating that the **L−M−L** linkages are hydrolyzable yet do not limit the lifetimes of these polymers in an aqueous environment. Similarly, the resonance of the syringic acid methoxy protons, initially a singlet at 3.8 ppm, developed a shoulder peak at 3.9 ppm at the very end of the film's lifetime, indicating that the **L−Sy−L** linkages are slower to cleave than the pentameric LG sequences.

Molecular Weight and Mass Loss. In the first 3 weeks of degradation, the two copolymers behaved similarly in molecular weight loss and mass loss (Figure 5). At week 4, the degradation profiles become distinct as a sharp drop in the controlled random copolymer's molecular weight results in a larger increase in mass loss, while the precisely sequenced copolymer drops at a more gradual rate. This faster mass loss for the controlled random copolymer is consistent with the formation of a high fraction of short-chain byproducts, similar to the behavior seen in the fully random PLGAs.[78]

Thermal Behavior. The thermal characteristics of the two polymers were monitored by differential scanning calorimetry during the hydrolysis study (Figure 6). Thermograms were collected on the first heating cycle to obtain native thermal features at a given time point. The initial thermograms of the polymers (week 0) display identical glass transition temperatures at 50 °C, as expected from the Flory−Fox equation, given their identical monomer composition.[73] Initially, neither displayed crystallization nor melting transitions. Slight degradation of the controlled random copolymer, however, resulted in the development of sharp, low-temperature melting transitions near 60 °C. In the sequenced copolymer, no melting transitions are observed, and the T_g remains at 50 °C. It should be noted that the unusual shape of the glass transitions is due to an increased short-range ordering of chains upon aging, which leads to enthalpic relaxation.[79] The optical transparency of the films correlates well with the thermograms—both films are transparent at week 0 and the controlled random becomes opaque by week 1 just as melting transitions appear (Figure 8). The sequenced films remain mostly transparent until approximately week 7 of hydrolysis.

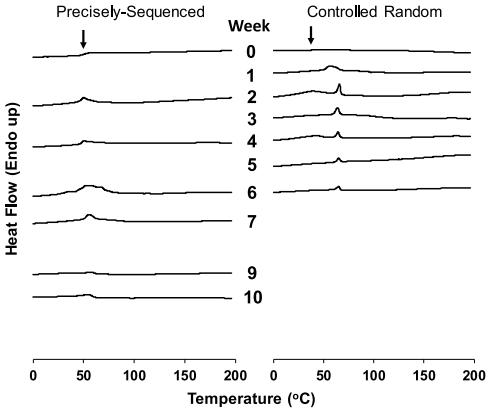

Figure 6. Differential scanning calorimetry thermograms of both sequenced and controlled random copolymers over the course of hydrolysis. Arrows indicate initial T_gs.

Film Characteristics. The surface features of the thick films were imaged by scanning electron microscopy. Low-magnification images (100×) showed that the sequenced polymer maintained its native surface uniformity throughout degradation and underwent clean fractures. The controlled random, however, exhibited immediate changes in surface appearance upon hydrolysis and degraded nonuniformly with the development of large voids and micron-sized pores (Figure 7). The bulk portions of films remaining at the end of hydrolysis were flakey and soft, differing from the small, dense particles left for the sequenced copolymer films (Figure 8).

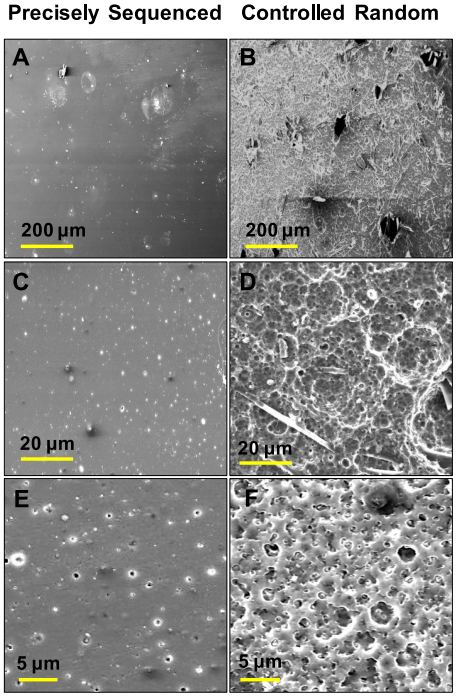

Figure 7. Scanning electron microscopy images (secondary ion detection, 10 keV) of polymer films over the course of hydrolysis. (A) **Poly SyLM(LGLGL)** at week 7, ∼50% loss of M_n, 100×. (B) **Poly SyLM(L_3G_2)** at week 4, ∼50% loss of M_n, 100×. (C) **Poly SyLM(LGLGL)** at week 7, 1000×. (D) **Poly SyLM(L_3G_2)** at week 4, 1000×. (E) **Poly SyLM(LGLGL)** at week 10, 3000×. (F) **Poly SyLM(L_3G_2)** at week 6, 3000×. Note the presence of residual buffer salt crystals in SEM-D.

DOI: 10.1021/acs.macromol.9b00480
Macromolecules 2019, 52, 4694−4702

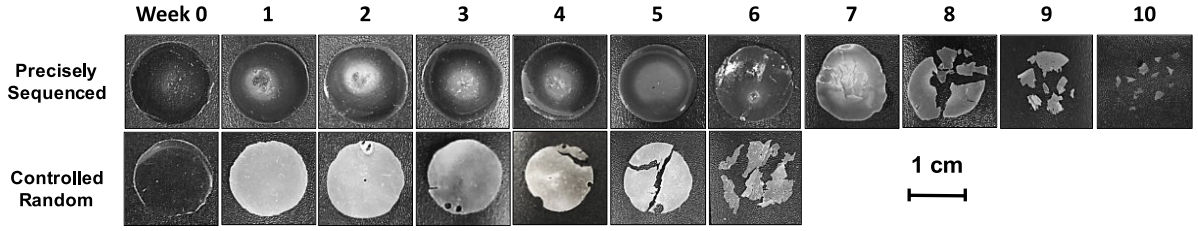

Figure 8. Photographs of copolymer thick films over the course of hydrolysis.

The brittle fracture pattern observed for the precisely sequenced copolymer can be explained by the increasing order of the chains during aging.[79] This explanation correlates well with the increased enthalpic relaxation observed in the thermograms.

DISCUSSION

Although we have established previously and observed in this study that hydrolysis behaviors are extremely sensitive to sequence, we note that not all polymer properties are as sequence-dependent. Specifically, for PLGAs, we have found that the prehydrolysis bulk and thermal properties are largely independent of monomer sequencing.[63,66] For instance, while one might expect that the highly ordered structure of a precise polymer could affect the T_g or crystallinity, we have generally observed that polyesters of identical composition but different sequencing display differences in T_g that are so small as to be difficult to differentiate from those that could be attributed to minor variations in molecular weight, thermal history, and plasticization due to humidity.[64,65] Moreover, despite the high degree of order in the backbone, the periodically sequenced copolymers are often poorly crystalline or amorphous. It is not surprising, therefore, that sequence errors do not result in significant differences in the degree of crystallinity.

In contrast with the thermal properties, we have found that the course of hydrolysis is extremely sequence-dependent as are the properties of the partially degraded copolymers at each time point. We have shown in our prior studies on related PLGAs that the hydrolytic degradation can be correlated with differences in bond cleavage rates of the monomers, which, in turn, affect the predominant mechanism of degradation.[62,64] Bond cleavage in polymer backbones generally proceeds by two mechanisms, intrachain scission, in which a bond is broken in the middle of a chain, and end-chain scission, which most commonly involves back-biting by a reactive end group.[80] Though both mechanisms act concurrently, the prevalence of one mechanism over the other results in distinctive molecular weight and mass loss profiles.[78] In a primarily chain-end degradation mechanism, molecular weight decreases linearly with accompanying small increases in dispersity. As small molecule byproducts are eliminated, the mass decreases gradually. However, when even a small degree of intrachain scission occurs, rapid molecular weight loss and large increases in dispersity result. Additionally, the fraction of small-chain oligomers that may be eliminated from the polymer matrix rapidly increases, causing a faster mass loss than would be observed for a sample in which chain-end degradation dominates.

We have previously shown, for example, that a simply alternating copolymer, $(LG)_n$, which we name **Poly LG**, exhibits chain-end hydrolysis as its primary mechanism, whereas the random analog of the same composition, **PDLGA-50**, shows significant intrachain cleavage during hydrolysis. This change can be logically correlated with the known kinetic differences in the reactivity with water of the various linkages: G−G > G−L, L−G > L−L.[62] In **PDLGA-50**, the fast-cleaving G−G linkages appear to lead to significant intrachain scission. That being said, it was not clear that G−G cleavage rates were the only factor that affected the hydrolysis profile. A major goal of the current study was, therefore, to isolate short-range monomer connectivity kinetics from other possible contributions, like stereochemistry and micro- or nanophase separation that could occur in the random copolymer, given the likely presence of longer L-rich and G-rich regions in the statistical chains.

Despite their relatively high degree of homology, differences during hydrolysis between **Poly SyLM(LGLGL)** and **Poly SyLM(L_3G_2)** mimic the scission patterns observed for **Poly LG** and **PDLGA-50**. Based on the rapid increase in dispersity, more rapid mass loss, and the development of low-temperature melting transitions, it is clear that the controlled random copolymer produces a larger fraction of small-chain oligomers and that the degradation involves significant intrachain scission.[47] For the sequenced copolymer in this work, the lesser and more gradual increase in dispersity and the more gradual mass loss suggest that less intrachain scission occurs during hydrolysis.

We also observe a strong effect of the monomer scrambling in the structure of the films during hydrolysis. In particular, the pore pattern that is observed in the SEM images of the controlled random polymer is consistent with the proposed predominance of intrachain scission cleaving G−G linkages to produce a heterogeneous pattern. Interestingly, however, **PDLGA-50**, which also comprises L- and G-rich regions, does not exhibit an analogous pore structure during degradation but instead plasticizes extensively to give a visually unstructured surface at the 1−10 μm scale.[77] We hypothesize that this difference is a result of the presence of the conformationally rigid and slower-degrading Sy−L−M linkages after every five monomer units, which limits the population and frequency of hydrolytically susceptible G−G linkages locally within the chain. Moreover, when combined with the randomly occurring L-rich segments, the range of differences in hydrolysis kinetics between regions is accentuated relative to the fully random PLGA. We note that the porous degradation structure observed for the controlled random copolymer could prove useful for applications in which the structural integrity of scaffolding needs to be preserved for as long as possible during degradation.

Having previously identified the effectiveness of G−G linkages in altering the hydrolysis behaviors of PLGAs, we originally sought to investigate the magnitude of general sequence sensitivity, as a sequenced PLGA becomes slightly randomized. In this study, we observed that PLGA-inspired

DOI: 10.1021/acs.macromol.9b00480
Macromolecules 2019, 52, 4694−4702

polyesters are incredibly sensitive to the precision of a short-range monomer order, having found that hydrolysis behaviors are changed dramatically by only a small degree of sequence scrambling. The synthetic method we employed effectively capped single monomer repetitions to five units. Therefore, the preparation of a precisely sequenced and a controlled random analog represents only a slight shift in the sequenced/randomized continuum (Figure 1, bottom curve).

CONCLUSIONS

To address the tolerance of properties to short-range sequence scrambling, we used ED-ROMP to prepare a precisely sequenced polyester comprising lactic, glycolic, and syringic acids along with a copolymer with an identical monomer composition but a slightly scrambled monomer sequence. Hydrolysis behaviors were monitored over time to reveal drastic contrasts despite a relatively small difference in precision sequencing. Molecular weight loss was accelerated within the controlled random copolymer, and dispersity measurements were consistent with an increased rate of intrachain scission versus the precisely sequenced copolymer. Microscopic pores and larger voids developed within the controlled random copolymer, whereas the precisely sequenced copolymer retained its native surface features to a larger degree throughout the course of degradation.

Lastly, while there exist many comonomer systems to prepare materials with targeted applications, the sequence remains an exciting tool for expanding the functional capacity of any given set of comonomers. While the synthesis continues to be a bottleneck in the preparation of sequenced materials, semisequencing may be used to avoid overly laborious syntheses. We are continuing our efforts in understanding how sequence errors affect behavior and in identifying properties that depend on sequence but can tolerate error.

ASSOCIATED CONTENT

Supporting Information

The Supporting Information is available free of charge on the ACS Publications website at DOI: 10.1021/acs.macromol.9b00480.

Drop-cast film thickness measurement (Figures S1 and S2); low-magnification (100×) images (Figure S3); high magnification (1000×) (Figure S4); high magnification (3000×) of the porous structure (Figure S5); differential scanning calorimetry thermogram (Figures S6 and S7); size exclusion chromatographs (Figures S8 and S9); and energy-dispersive X-ray characterization of residual buffer salt crystals (Figure S10) (PDF)

AUTHOR INFORMATION

Corresponding Author

*E-mail: tmeyer@pitt.edu. Tel: 412-624-8635.

ORCID

Tara Y. Meyer: 0000-0002-9810-454X

Notes

The authors declare no competing financial interest.

ACKNOWLEDGMENTS

The authors acknowledge the NSF CHE-1709144, CHE-1625002 for MALDI-ToF instrumentation, and the University of Pittsburgh for financial support.

REFERENCES

(1) Tsuchiya, K.; Ishii, T.; Masunaga, H.; Numata, K. Spider dragline silk composite films doped with linear and telechelic polyalanine: Effect of polyalanine on the structure and mechanical properties. *Sci. Rep.* **2018**, *8*, No. 3654.

(2) Rising, A.; Johansson, J. Toward spinning artificial spider silk. *Nat. Chem. Biol.* **2015**, *11*, 309.

(3) Heim, M.; Keerl, D.; Scheibel, T. Spider Silk: From Soluble Protein to Extraordinary Fiber. *Angew. Chem., Int. Ed.* **2009**, *48*, 3584−3596.

(4) Lutz, J.-F. Defining the Field of Sequence-Controlled Polymers. *Macromol. Rapid Commun.* **2017**, *38*, No. 1700582.

(5) Lutz, J.-F.; Ouchi, M.; Liu, D. R.; Sawamoto, M. Sequence-Controlled Polymers. *Science* **2013**, *341*, No. 1238149.

(6) Swisher, J. H. N.; Jamie, A.; Washington, M. A.; Meyer, T. Y. Properties and Applications of Sequence-Controlled Polymers; In *Sequence-Controlled Polymers*; Lutz, J.-F., Ed.; Wiley: 2017.

(7) Zhang, J.; Matta, M. E.; Hillmyer, M. A. Synthesis of Sequence-Specific Vinyl Copolymers by Regioselective ROMP of Multiply Substituted Cyclooctenes. *ACS Macro Lett.* **2012**, *1*, 1383−1387.

(8) Li, G.; Sampson, N. S. Alternating Ring-Opening Metathesis Polymerization (AROMP) of Hydrophobic and Hydrophilic Monomers Provides Oligomers with Side-Chain Sequence Control. *Macromolecules* **2018**, 3932.

(9) Parker, K. A.; Sampson, N. S. Precision Synthesis of Alternating Copolymers via Ring-Opening Polymerization of 1-Substituted Cyclobutenes. *Acc. Chem. Res.* **2016**, *49*, 408−417.

(10) Badi, N.; Lutz, J.-F. Sequence control in polymer synthesis. *Chem. Soc. Rev.* **2009**, *38*, 3383−3390.

(11) Lutz, J.-F.; Ouchi, M.; Sawamoto, M.; Meyer, T. Y. *Sequence-Controlled Polymers: Synthesis, Self-Assembly, and Properties*; American Chemical Society, 2014; Vol. *1170*.

(12) Simocko, C.; Young, T. C.; Wagener, K. B. ADMET Polymers Containing Precisely Spaced Pendant Boronic Acids and Esters. *Macromolecules* **2015**, *48*, 5470−5473.

(13) Rojas, G.; Wagener, K. B. Precisely and Irregularly Sequenced Ethylene/1-Hexene Copolymers: A Synthesis and Thermal Study. *Macromolecules* **2009**, *42*, 1934−1947.

(14) Gutekunst, W. R.; Hawker, C. J. A General Approach to Sequence-Controlled Polymers Using Macrocyclic Ring Opening Metathesis Polymerization. *J. Am. Chem. Soc.* **2015**, *137*, 8038−8041.

(15) Fu, C.; Huang, Z.; Hawker, C. J.; Moad, G.; Xu, J.; Boyer, C. RAFT-mediated, visible light-initiated single unit monomer insertion and its application in the synthesis of sequence-defined polymers. *Polym. Chem.* **2017**, *8*, 4637−4643.

(16) Cole, J. P.; Lessard, J. J.; Rodriguez, K. J.; Hanlon, A. M.; Reville, E. K.; Mancinelli, J. P.; Berda, E. B. Single-chain nanoparticles containing sequence-defined segments: using primary structure control to promote secondary and tertiary structures in synthetic protein mimics. *Polym. Chem.* **2017**, *8*, 5829−5835.

(17) Soejima, T.; Satoh, K.; Kamigaito, M. Sequence-regulated vinyl copolymers with acid and base monomer units via atom transfer radical addition and alternating radical copolymerization. *Polym. Chem.* **2016**, *7*, 4833−4841.

(18) Soejima, T.; Satoh, K.; Kamigaito, M. Main-Chain and Side-Chain Sequence-Regulated Vinyl Copolymers by Iterative Atom Transfer Radical Additions and 1:1 or 2:1 Alternating Radical Copolymerization. *J. Am. Chem. Soc.* **2016**, *138*, 944−954.

(19) Lu, X.; Watts, E.; Jia, F.; Tan, X.; Zhang, K. Polycondensation of Polymer Brushes via DNA Hybridization. *J. Am. Chem. Soc.* **2014**, *136*, 10214−10217.

(20) Sigle, J. L.; Clough, A.; Zhou, J.; White, J. L. Controlling Macroscopic Properties by Tailoring Nanoscopic Interfaces in Tapered Copolymers. *Macromolecules* **2015**, *48*, 5714−5722.

(21) Luo, M.; Brown, J. R.; Remy, R. A.; Scott, D. M.; Mackay, M. E.; Hall, L. M.; Epps, T. H. Determination of Interfacial Mixing in Tapered Block Polymer Thin Films: Experimental and Theoretical Investigations. *Macromolecules* **2016**, *49*, 5213−5222.

DOI: 10.1021/acs.macromol.9b00480
Macromolecules 2019, 52, 4694−4702

(22) O'Connor, K. S.; Watts, A.; Vaidya, T.; LaPointe, A. M.; Hillmyer, M. A.; Coates, G. W. Controlled Chain Walking for the Synthesis of Thermoplastic Polyolefin Elastomers: Synthesis, Structure, and Properties. *Macromolecules* **2016**, *49*, 6743−6751.
(23) Tang, D.; Chen, Z.; Correa-Netto, F.; Macosko, C. W.; Hillmyer, M. A.; Zhang, G. Poly(urea ester): A family of biodegradable polymers with high melting temperatures. *J. Polym. Sci., Part A: Polym. Chem.* **2016**, *54*, 3795−3799.
(24) Chile, L.-E.; Mehrkhodavandi, P.; Hatzikiriakos, S. G. A Comparison of the Rheological and Mechanical Properties of Isotactic, Syndiotactic, and Heterotactic Poly(lactide). *Macromolecules* **2016**, *49*, 909−919.
(25) Cole, J. P.; Hanlon, A. M.; Rodriguez, K. J.; Berda, E. B. Protein-like structure and activity in synthetic polymers. *J. Polym. Sci., Part A: Polym. Chem.* **2017**, *55*, 191−206.
(26) Romulus, J.; Weck, M. Single-Chain Polymer Self-Assembly Using Complementary Hydrogen Bonding Units. *Macromol. Rapid Commun.* **2013**, *34*, 1518−1523.
(27) Zhang, J.; Landry, M. P.; Barone, P. W.; Kim, J.-H.; Lin, S.; Ulissi, Z. W.; Lin, D.; Mu, B.; Boghossian, A. A.; Hilmer, A. J.; Rwei, A.; Hinckley, A. C.; Kruss, S.; Shandell, M. A.; Nair, N.; Blake, S.; Sen, F.; Sen, S.; Croy, R. G.; Li, D.; Yum, K.; Ahn, J.-H.; Jin, H.; Heller, D. A.; Essigmann, J. M.; Blankschtein, D.; Strano, M. S. Molecular recognition using corona phase complexes made of synthetic polymers adsorbed on carbon nanotubes. *Nat. Nanotechnol.* **2013**, *8*, 959−968.
(28) Grate, J. W.; Mo, K.-F.; Daily, M. D. Triazine-Based Sequence-Defined Polymers with Side-Chain Diversity and Backbone−Backbone Interaction Motifs. *Angew. Chem., Int. Ed.* **2016**, *55*, 3925−3930.
(29) Mahon, C. S.; Fulton, D. A. Mimicking nature with synthetic macromolecules capable of recognition. *Nat. Chem.* **2014**, *6*, 665−672.
(30) Lavilla, C.; Byrne, M.; Heise, A. Block-Sequence-Specific Polypeptides from α-Amino Acid N-Carboxyanhydrides: Synthesis and Influence on Polypeptide Properties. *Macromolecules* **2016**, *49*, 2942−2947.
(31) Knight, A. S.; Zhou, E. Y.; Francis, M. B.; Zuckermann, R. N. Sequence Programmable Peptoid Polymers for Diverse Materials Applications. *Adv. Mater.* **2015**, *27*, 5665−5691.
(32) Shin, H.-M.; Kang, C.-M.; Yoon, M.-H.; Seo, J. Peptoid helicity modulation: precise control of peptoid secondary structures via position-specific placement of chiral monomers. *Chem. Commun.* **2014**, *50*, 4465−4468.
(33) Bergman, J. A.; Cochran, E. W.; Heinen, J. M. Role of the segment distribution in the microphase separation of acrylic diblock and triblock terpolymers. *Polymer* **2014**, *55*, 4206−4215.
(34) Tsai, C.-H.; Fortney, A.; Qiu, Y.; Gil, R. R.; Yaron, D.; Kowalewski, T.; Noonan, K. J. T. Conjugated Polymers with Repeated Sequences of Group 16 Heterocycles Synthesized through Catalyst-Transfer Polycondensation. *J. Am. Chem. Soc.* **2016**, *138*, 6798−6804.
(35) Wada, Y.; Lee, H.; Hoshino, Y.; Kotani, S.; Shea, K. J.; Miura, Y. Design of multi-functional linear polymers that capture and neutralize a toxic peptide: a comparison with cross-linked nanoparticles. *J. Mater. Chem. B* **2015**, *3*, 1706−1711.
(36) Chen, Y.; Liu, T.; Xu, G.; Zhang, J.; Zhai, X.; Yuan, J.; Tan, Y. Aggregation behavior of X-shaped branched block copolymers at the air/water interface: effect of block sequence and temperature. *Colloid Polym. Sci.* **2015**, *293*, 97−107.
(37) Robinson, D. B.; Buffleben, G. M.; Langham, M. E.; Zuckermann, R. N. Stabilization of nanoparticles under biological assembly conditions using peptoids. *Biopolymers* **2011**, *96*, 669−678.
(38) Pesko, D. M.; Webb, M. A.; Jung, Y.; Zheng, Q.; Miller, T. F.; Coates, G. W.; Balsara, N. P. Universal Relationship between Conductivity and Solvation-Site Connectivity in Ether-Based Polymer Electrolytes. *Macromolecules* **2016**, *49*, 5244−5255.
(39) Luo, S.; Stevens, K. A.; Park, J. S.; Moon, J. D.; Liu, Q.; Freeman, B. D.; Guo, R. Highly CO2-Selective Gas Separation Membranes Based on Segmented Copolymers of Poly(Ethylene oxide) Reinforced with Pentiptycene-Containing Polyimide Hard Segments. *ACS Appl. Mater. Interfaces* **2016**, *8*, 2306−2317.
(40) Sun, J.; Teran, A. A.; Liao, X.; Balsara, N. P.; Zuckermann, R. N. Crystallization in Sequence-Defined Peptoid Diblock Copolymers Induced by Microphase Separation. *J. Am. Chem. Soc.* **2014**, *136*, 2070−2077.
(41) Panganiban, B.; Qiao, B.; Jiang, T.; DelRe, C.; Obadia, M. M.; Nguyen, T. D.; Smith, A. A. A.; Hall, A.; Sit, I.; Crosby, M. G.; Dennis, P. B.; Drockenmuller, E.; Olvera de la Cruz, M.; Xu, T. Random heteropolymers preserve protein function in foreign environments. *Science* **2018**, *359*, 1239−1243.
(42) Trigg, E. B.; Tiegs, B. J.; Coates, G. W.; Winey, K. I. High Morphological Order in a Nearly Precise Acid-Containing Polymer and Ionomer. *ACS Macro Lett.* **2017**, *6*, 947−951.
(43) Howard, J. B.; Ekiz, S.; Cuellar De Lucio, A. J.; Thompson, B. C. Investigation of Random Copolymer Analogues of a Semi-Random Conjugated Polymer Incorporating Thieno[3,4-b]pyrazine. *Macromolecules* **2016**, *49*, 6360−6367.
(44) Singh, N.; Tureau, M. S.; Epps, I. I. I. T. H. Manipulating ordering transitions in interfacially modified block copolymers. *Soft Matter* **2009**, *5*, 4757−4762.
(45) Versteegen, R. M.; Sijbesma, R. P.; Meijer, E. W. Synthesis and Characterization of Segmented Copoly(ether urea)s with Uniform Hard Segments. *Macromolecules* **2005**, *38*, 3176−3184.
(46) Anderson, J. M.; Shive, M. S. Biodegradation and biocompatibility of PLA and PLGA microspheres. *Adv. Drug Delivery Rev.* **1997**, *28*, 5−24.
(47) Batycky, R. P.; Hanes, J.; Langer, R.; Edwards, D. A. A Theoretical Model of Erosion and Macromolecular Drug Release from Biodegrading Microspheres. *J. Pharm. Sci.* **1997**, *86*, 1464−1477.
(48) Farahani, T. D.; Akbar Entezami, A.; Mobedi, H.; Abtahi, M. Degradation of Poly(D,L-lactide-co-glycolide) 50:50 Implant in Aqueous Medium. *Iran. Polym. J.* **2005**, *14*, 753−763.
(49) Shi, X.; Wang, Y.; Ren, L.; Gong, Y.; Wang, D.-A. Enhancing Alendronate Release from a Novel PLGA/Hydroxyapatite Microspheric System for Bone Repairing Applications. *Pharm. Res.* **2009**, *26*, 422−430.
(50) Makadia, H. K.; Siegel, S. J. Poly Lactic-co-Glycolic Acid (PLGA) as Biodegradable Controlled Drug Delivery Carrier. *Polymers* **2011**, *3*, 1377−1397.
(51) Pan, Z.; Ding, J. Poly(lactide-co-glycolide) porous scaffolds for tissue engineering and regenerative medicine. *Interface Focus* **2012**, *2*, 366−377.
(52) Gentile, P.; Chiono, V.; Carmagnola, I.; Hatton, V. P. An Overview of Poly(lactic-co-glycolic) Acid (PLGA)-Based Biomaterials for Bone Tissue Engineering. *Int. J. Mol. Sci.* **2014**, *15*, 3640−3659.
(53) Kapoor, D. N.; Bhatia, A.; et al. PLGA: a unique polymer for drug delivery. *Ther. Delivery* **2015**, *6*, 41−58.
(54) Shibata, A.; Machida, M.; Kondo, N.; Terakawa, M. Biodegradability of poly(lactic-co-glycolic acid) and poly(l-lactic acid) after deep-ultraviolet femtosecond and nanosecond laser irradiation. *Appl. Phys. A* **2017**, *123*, 438.
(55) Lambert, S.; Wagner, M. Environmental performance of bio-based and biodegradable plastics: the road ahead. *Chem. Soc. Rev.* **2017**, *46*, 6855−6871.
(56) Brannigan, R. P.; Dove, A. P. Synthesis, properties and biomedical applications of hydrolytically degradable materials based on aliphatic polyesters and polycarbonates. *Biomater. Sci.* **2017**, *5*, 9−21.
(57) Lambert, S.; Wagner, M. Environmental performance of bio-based and biodegradable plastics: the road ahead. *Chem. Soc. Rev.* **2017**, 6855.
(58) Laycock, B.; Nikolić, M.; Colwell, J. M.; Gauthier, E.; Halley, P.; Bottle, S.; George, G. Lifetime prediction of biodegradable polymers. *Prog. Polym. Sci.* **2017**, *71*, 144−189.
(59) Washington, M. A.; Balmert, S. C.; Fedorchak, M. V.; Little, S. R.; Watkins, S. C.; Meyer, T. Y. Monomer sequence in PLGA microparticles: Effects on acidic microclimates and in vivo inflammatory response. *Acta Biomater.* **2018**, *65*, 259−271.

DOI: 10.1021/acs.macromol.9b00480
Macromolecules 2019, 52, 4694−4702

(60) Short, A. L.; Fang, C.; Nowalk, J. A.; Weiss, R. M.; Liu, P.; Meyer, T. Y. Cis-Selective Metathesis to Enhance the Living Character of Ring-Opening Polymerization: An Approach to Sequenced Copolymers. *ACS Macro Lett.* **2018**, *7*, 858−862.
(61) Weiss, R. M.; Li, J.; Liu, H. H.; Washington, M. A.; Giesen, J. A.; Grayson, S. M.; Meyer, T. Y. Determining Sequence Fidelity in Repeating Sequence Poly(lactic-co-glycolic acid)s. *Macromolecules* **2017**, *50*, 550−560.
(62) Washington, M. A.; Swiner, D. J.; Bell, K. R.; Fedorchak, M. V.; Little, S. R.; Meyer, T. Y. The impact of monomer sequence and stereochemistry on the swelling and erosion of biodegradable poly(lactic-co-glycolic acid) matrices. *Biomaterials* **2017**, *117*, 66−76.
(63) Weiss, R. M.; Short, A. L.; Meyer, T. Y. Sequence-Controlled Copolymers Prepared via Entropy-Driven Ring-Opening Metathesis Polymerization. *ACS Macro Lett.* **2015**, *4*, 1039−1043.
(64) Li, J.; Rothstein, S. N.; Little, S. R.; Edenborn, H. M.; Meyer, T. Y. The Effect of Monomer Order on the Hydrolysis of Biodegradable Poly(lactic-co-glycolic acid) Repeating Sequence Copolymers. *J. Am. Chem. Soc.* **2012**, *134*, 16352−16359.
(65) Weiss, R. M.; Jones, E. M.; Shafer, D. E.; Stayshich, R. M.; Meyer, T. Y. Synthesis of repeating sequence copolymers of lactic, glycolic, and caprolactic acids. *J. Polym. Sci., Part A: Polym. Chem.* **2011**, *49*, 1847−1855.
(66) Stayshich, R. M.; Meyer, T. Y. New Insights into Poly(lactic-co-glycolic acid) Microstructure: Using Repeating Sequence Copolymers To Decipher Complex NMR and Thermal Behavior. *J. Am. Chem. Soc.* **2010**, *132*, 10920−10934.
(67) Zhang, S.; Bauer, N. E.; Kanal, I. Y.; You, W.; Hutchison, G. R.; Meyer, T. Y. Sequence Effects in Donor−Acceptor Oligomeric Semiconductors Comprising Benzothiadiazole and Phenylenevinylene Monomers. *Macromolecules* **2017**, *50*, 151−161.
(68) Bischof, A. M.; Zhang, S.; Meyer, T. Y.; Lear, B. J. Quantitative Assessment of the Connection between Steric Hindrance and Electronic Coupling in 2,5-Bis(alkoxy)benzene-Based Mixed-Valence Dimers. *J. Phys. Chem. C* **2014**, *118*, 12693−12699.
(69) Thorn-Csányi, E.; Ruhland, K. Quantitative description of the metathesis polymerization/depolymerization equilibrium in the 1,4-polybutadiene system, 3. Influence of the solvent. *Macromol. Chem. Phys.* **1999**, *200*, 2606−2611.
(70) Peng, Y.; Decatur, J.; Meier, M. A. R.; Gross, R. A. Ring-Opening Metathesis Polymerization of a Naturally Derived Macrocyclic Glycolipid. *Macromolecules* **2013**, *46*, 3293−3300.
(71) Pepels, M. P. F.; Souljé, P.; Peters, R.; Duchateau, R. Theoretical and Experimental Approach to Accurately Predict the Complex Molecular Weight Distribution in the Polymerization of Strainless Cyclic Esters. *Macromolecules* **2014**, *47*, 5542−5550.
(72) Nowalk, J. A.; Fang, C.; Short, A. L.; Weiss, R. M.; Swisher, J. H.; Liu, P.; Meyer, T. Y. Sequence-Controlled Polymers Through Entropy-Driven Ring-Opening Metathesis Polymerization: Theory, Molecular Weight Control, and Monomer Design. *J. Am. Chem. Soc.* **2019**, *141*, 5741−5752.
(73) Swisher, J. H.; Nowalk, J. A.; Meyer, T. Y. Property impact of common linker segments in sequence-controlled polyesters. *Polym. Chem.* **2019**, 244−252.
(74) Nguyen, H. T. H.; Short, G. N.; Qi, P.; Miller, S. A. Copolymerization of lactones and bioaromatics via concurrent ring-opening polymerization/polycondensation. *Green Chem.* **2017**, 1877−1888.
(75) Short, G. N.; Nguyen, H. T. H.; Scheurle, P. I.; Miller, S. A. Aromatic polyesters from biosuccinic acid. *Polym. Chem.* **2018**, *9*, 4113−4119.
(76) Shirazi, R. N.; Aldabbagh, F.; Erxleben, A.; Rochev, Y.; McHugh, P. Nanomechanical properties of poly(lactic-co-glycolic) acid film during degradation. *Acta Biomater.* **2014**, *10*, 4695−4703.
(77) Lu, L.; Garcia, C. A.; Mikos, A. G. In vitro degradation of thin poly(DL-lactic-co-glycolic acid) films. *J. Biomed. Mater. Res.* **1999**, *46*, 236−244.
(78) Gleadall, A.; Pan, J.; Kruft, M.-A.; Kellomäki, M. Degradation mechanisms of bioresorbable polyesters. Part 1. Effects of random scission, end scission and autocatalysis. *Acta Biomater.* **2014**, *10*, 2223−2232.
(79) Pan, P.; Zhu, B.; Inoue, Y. Enthalpy Relaxation and Embrittlement of Poly(l-lactide) during Physical Aging. *Macromolecules* **2007**, *40*, 9664−9671.
(80) Ho, Y. K.; Doshi, P.; Yeoh, H. K.; Ngoh, G. C. Modeling chain-end scission using the Fixed Pivot technique. *Chem. Eng. Sci.* **2014**, *116*, 601−610.

DOI: 10.1021/acs.macromol.9b00480
Macromolecules 2019, 52, 4694−4702